

# Sources of n-type conductivity in ZnO

M.D. McCluskey\*, S.J. Jokela

*Department of Physics and Astronomy, Washington State University, Pullman, WA 99164-2814, USA*

## Abstract

Zinc oxide (ZnO) is a strong candidate for energy-efficient white lighting and numerous optoelectronic applications. Hydrogen impurities play important roles, good and bad, in the pursuit of reliable p-type doping of ZnO. In previous work, we identified hydrogen donors with the back-bonded or “anti-bonding” orientation, with an angle of  $111^\circ$  to the *c*-axis. It is possible, however, that these hydrogen donors are complexed with another defect. Impurities besides hydrogen are also donors in as-grown ZnO. Results from secondary ion mass spectroscopy (SIMS) show significant concentrations of Al in samples of bulk single-crystal ZnO obtained from Cermet, Inc., Ga and B in samples from Eagle-Picher, and Si in both.

© 2007 Elsevier B.V. All rights reserved.

*Keywords:* Hydrogen; Infrared; ZnO; SIMS

## 1. Introduction

Owing to its high quantum efficiency, band gap of 3.3 eV, and environmentally friendly composition, zinc oxide (ZnO) is a strong candidate for energy-efficient lighting applications. Unlike gallium nitride (GaN), large single crystals can be grown [1]. ZnO is already utilized as a transparent conductor [2] in solar cells [3] and is a leading material for transparent transistors [4]. Unless reliable p-type doping can be achieved, however, ZnO will not become economically competitive with semiconductors like GaN. To solve that problem, the role of donor impurities needs to be understood. In this paper, we summarize the results of infrared (IR) and compositional studies designed to determine sources of n-type conductivity in ZnO.

One important donor in ZnO is hydrogen. The early work of Mollwo [5] and Thomas and Lander [6] demonstrated that hydrogen diffused into ZnO increased the n-type conductivity of the sample. Several decades later, first-principles calculations by Van de Walle [7] showed that hydrogen was a donor in ZnO. Proposed models for the O–H donors are shown in Fig. 1, the back-bonded or “anti-bonding” ( $AB_{\perp}$ ) configuration and the bond-centered ( $BC_{\parallel}$ ) configuration. Other models include the  $AB_{\parallel}$

and  $BC_{\perp}$  configurations. Motivated by this work, experiments on muonium-implanted ZnO [8] and electron-nuclear resonance studies on n-type ZnO [9] provided evidence that hydrogen was indeed a shallow donor.

To determine the actual structure of hydrogen donors, IR spectroscopy was used to observe local vibrational modes (LVMs) arising from hydrogen-related complexes. We observed an O–H bond-stretching mode at  $3126\text{ cm}^{-1}$  at liquid-helium temperatures [10]. The frequency and hydrogen/deuterium shifts were consistent with O–H complexes. Further experiments [11], combined with first-principles calculations [12], provided evidence that the  $3126\text{ cm}^{-1}$  peak arises from hydrogen in the  $AB_{\perp}$  configuration.

This conclusion, however, appears to contradict other studies. IR measurements on ZnO grown by vapor-transport showed a mode at  $3611\text{ cm}^{-1}$ , consistent with the  $BC_{\parallel}$  model [13]. In addition, a study of muonium in ZnO claimed that the complexes are aligned parallel to the *c*-axis [14]. Alvin Shi et al. [15] showed that samples from Cermet, Inc. showed a strong  $3126\text{ cm}^{-1}$  peak and a weak  $3611\text{ cm}^{-1}$  peak, and vice versa for Eagle-Picher samples. These findings suggest that observed hydrogen modes may arise from defect-hydrogen complexes. The concentration of defects present in as-grown material could determine the relative populations of the  $3126$  and  $3611\text{ cm}^{-1}$  hydrogen-related complexes.

\*Corresponding author. Tel.: +1 509 335 5356; fax: +1 509 335 7816.  
E-mail address: [mattmcc@wsu.edu](mailto:mattmcc@wsu.edu) (M.D. McCluskey).

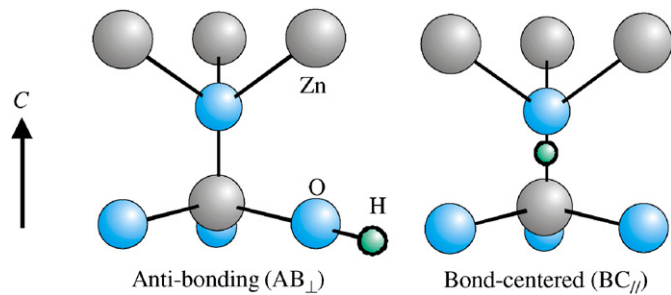


Fig. 1. Two models for hydrogen donors in ZnO.

While hydrogen is certainly a donor in ZnO, it is not the only one. It is known that group-III impurities such as Al and Ga are important sources of n-type conductivity [16]. To address issues related to hydrogen and other donors in ZnO, we performed secondary ion mass spectrometry (SIMS) and nuclear activation analysis (NAA) on samples provided by Cermet and Eagle-Picher.

## 2. Experiment

Bulk, single-crystal samples from Cermet, Inc. and Eagle-Picher were used in this study. The Cermet samples are grown by a pressurized melt-growth process [17], whereas the Eagle-Picher samples were grown by chemical vapor transport [18]. Hall-effect measurements were performed in the Van der Pauw geometry with silver contacts. The measurements showed free electron concentrations of  $(1.48 \pm 0.03) \times 10^{17} \text{ cm}^{-3}$  and  $(1.10 \pm 0.01) \times 10^{17} \text{ cm}^{-3}$  for the Cermet and Eagle-Picher samples, respectively.

Delayed gamma neutron activation analysis (DGNA) was performed using the 1MW General Atomics TRIGA nuclear reactor at Washington State University. The DGNA technique relies on the fact that certain stable isotopes can capture thermal neutrons and become radioactive. The radioactive atom then decays with a unique gamma-ray emission energy and half-life, providing a “fingerprint” for the element. Two samples, one produced by Eagle-Picher and the other produced by Cermet, Inc., were placed in the reactor along with two standards of known composition.

SIMS was performed by the Evans Analytical Group, using  $\text{O}_2^+$  and  $\text{Cs}^+$  primary ion beams with energies of 8 and 14.5 keV, respectively. The  $\text{O}_2^+$  beam is used for positive secondary ions (elements on the left side of the periodic table) and the  $\text{Cs}^+$  beam is used for negative secondary ions.

## 3. Results

The DGNA results are shown in Table 1. Although no impurities were detected in either sample, the results place upper bounds on potentially important impurities such as Ce, Co, and Mn. The difference in sensitivities between DGNA and SIMS arises, in part, from the fact that only

Table 1  
DGNA results for ZnO provided by Cermet and Eagle-Picher

Element	Concentration ( $\text{cm}^{-3}$ )
As	<3E16
Ce	<2E15
Co	<2E15
Cr	<1E16
Cs	<3E14
Dy	<4E15
Eu	<3E14
Fe	<1E18
Gd	<4E14
Hf	<3E14
K	<5E18
Lu	<1E14
Mn	<6E15
Na	<2E17
Rb	<4E16
Sb	<4E15
Sc	<1E14
Sm	<4E14
Sr	<3E17
Ta	<5E14
Tb	<3E14
Th	<2E14
Yb	<2E14

Concentrations are given in units of  $\text{atoms cm}^{-3}$ . The upper bounds apply to both samples.

Table 2  
SIMS results for ZnO provided by Cermet and Eagle-Picher

Element	Ion beam	Detection threshold $T$ ( $\text{cm}^{-3}$ )	Cermet ZnO ( $\text{cm}^{-3}$ )	Eagle-Picher ZnO ( $\text{cm}^{-3}$ )
Al	$\text{O}_2^+$	1E14	$(2.3 \pm 0.5)\text{E}17$	$(1.4 \pm 0.3)\text{E}15$
B	$\text{O}_2^+$	2E14	< $T$	$(2.5 \pm 0.5)\text{E}16$
C	$\text{Cs}^+$	3E18	< $T$	< $T$
Ca	$\text{O}_2^+$	7E14	$(4.0 \pm 1.6)\text{E}16$	< $T$
Cd	$\text{O}_2^+$	1E17	< $T$	< $T$
Cl	$\text{Cs}^+$	8E16	< $T$	< $T$
Cu	$\text{O}_2^+$	5E14	$\sim 1\text{E}15$	$\sim 1\text{E}15$
F	$\text{Cs}^+$	5E15	< $T$	< $T$
Ga	$\text{O}_2^+$	3E14	$\sim 1\text{E}15$	$\sim 1\text{E}16$
H	$\text{Cs}^+$	2E19	< $T$	< $T$
In	$\text{O}_2^+$	1E15	< $T$	< $T$
K	$\text{O}_2^+$	3E14	< $T$	< $T$
Li	$\text{O}_2^+$	3E13	$(8.5 \pm 3.4)\text{E}15$	< $T$
Mg	$\text{O}_2^+$	5E13	$(1.6 \pm 0.6)\text{E}16$	< $T$
N	$\text{Cs}^+$	2E16	< $T$	< $T$
Na	$\text{O}_2^+$	1E14	$(1.2 \pm 0.5)\text{E}15$	$(2.0 \pm 0.8)\text{E}14$
Si	$\text{Cs}^+$	5E15	$(1.0 \pm 0.2)\text{E}17$	$(1.3 \pm 0.3)\text{E}17$

certain naturally occurring isotopes give rise to a DGNA signal.

The SIMS results (Table 2) provide useful information about difference between Cermet and Eagle-Picher samples. Depth profiles are shown in Figs. 2 and 3. Cermet samples contain significant concentrations of Al ( $\sim 2 \times 10^{17} \text{ cm}^{-3}$ ). This level is comparable to the free

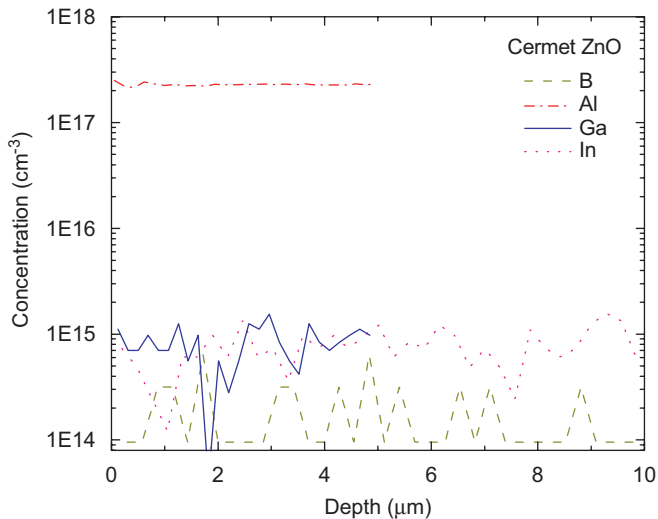


Fig. 2. SIMS depth profile of group-III impurities in Cermet ZnO.

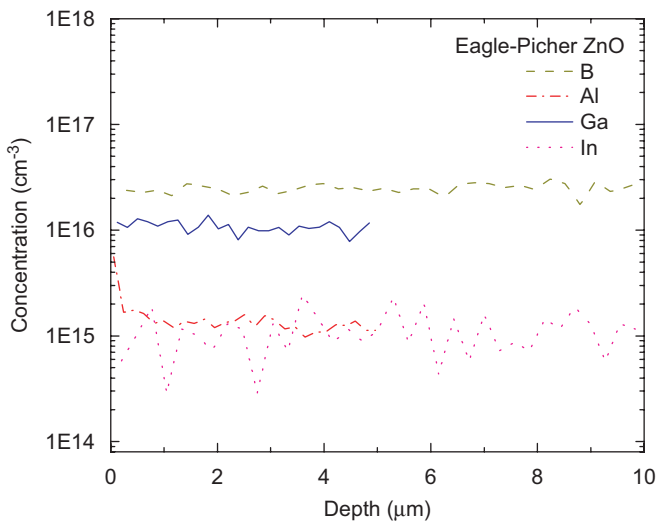


Fig. 3. SIMS depth profile of group-III impurities in Eagle-Picher ZnO.

electron concentration, suggesting that Al impurities are the dominant donors in Cermet ZnO samples. Eagle-Picher samples, in contrast, contain Ga and B impurities with concentrations  $\sim 10^{16} \text{ cm}^{-3}$ . Prior studies have shown that Eagle-Picher samples contain H donors with a concentration of  $\sim 10^{17} \text{ cm}^{-3}$  [9,19]. It is plausible that these H donors are in the form of hydrogen-decorated oxygen vacancies [20].

Cermet samples contain the group-II elements Ca and Mg with concentrations of  $\sim 10^{16} \text{ cm}^{-3}$ . It is possible that the O–H LVMs observed by Jokela and McCluskey [11] arise from complexes with these elements, although there is no definitive proof of this. Finally, both samples contained Cu impurities at the  $10^{15} \text{ cm}^{-3}$  level and Si impurities at the

$10^{17} \text{ cm}^{-3}$  level. While Cu is known to be an acceptor, the role of Si has not been investigated.

#### 4. Conclusions

The primary source of n-type conductivity in Cermet ZnO is likely Al, whereas Eagle-Picher samples contain comparable concentrations of B, Ga, and H donors. Both samples contain Si impurities. Cermet samples also contain the isoelectronic impurities Mg and Ca. The reason why hydrogen forms different IR-active complexes in the two samples is still unclear, although Mg–OH or Ca–OH complexes are possibilities.

#### Acknowledgments

The authors would like to thank Dan Dugan and James Elliston at the WSU Nuclear Radiation Center and Shaw Wang at the Evans Analytical Group. This work was supported by the National Science Foundation under Grant No. DMR-0704163.

#### References

- [1] J.M. Ntep, S.S. Hassani, A. Lusson, A. Tromson-Carli, D. Ballutaud, G. Didier, R. Triboulet, *J. Crystal Growth* 207 (1999) 30.
- [2] T. Minami, *MRS Bull.* 25 (8) (2000) 38.
- [3] A. Nuruddin, J.R. Abelson, *Thin Solid Films* 394 (2001) 49.
- [4] J.F. Wager, *Science* 300 (2003) 1245.
- [5] E. Mollwo, *Z. Phys.* 138 (1954) 478.
- [6] D.G. Thomas, J.J. Lander, *J. Chem. Phys.* 25 (1956) 1136.
- [7] C.G. Van de Walle, *Phys. Rev. Lett.* 85 (2000) 1012.
- [8] S.F.J. Cox, E.A. Davis, S.P. Cottrell, P.J.C. King, J.S. Lord, J.M. Gil, H.V. Alberto, R.C. Vilão, J. Piroto Duarte, N. Ayres de Campos, A. Weidinger, R.L. Lichti, S.J.C. Irvine, *Phys. Rev. Lett.* 86 (2001) 2601.
- [9] D.M. Hoffman, A. Hofstaetter, F. Leiter, H. Zhou, F. Henecker, B.K. Meyer, S.B. Orlinskii, J. Schmidt, P.G. Baranov, *Phys. Rev. Lett.* 88 (2002) 045504.
- [10] M.D. McCluskey, S.J. Jokela, K.K. Zhuravlev, P.J. Simpson, K.G. Lynn, *Appl. Phys. Lett.* 81 (2002) 3807.
- [11] S.J. Jokela, M.D. McCluskey, *Phys. Rev. B* 72 (2005) 113201.
- [12] S. Limpijumnong, S.B. Zhang, *Appl. Phys. Lett.* 86 (2005) 151910.
- [13] E.V. Lavrov, J. Weber, F. Börrnert, C.G. Van de Walle, R. Heilbig, *Phys. Rev. B* 66 (2002) 165205.
- [14] K. Shimomura, K. Nishiyama, R. Kadono, *Phys. Rev. Lett.* 89 (2002) 255505.
- [15] G. Alvin Shi, M. Stavola, S.J. Pearton, M. Thieme, E.V. Lavrov, J. Weber, *Phys. Rev. B* 72 (2005) 195211.
- [16] T. Minami, *MRS Bull.* 25 (8) (2000) 38.
- [17] D.C. Reynolds, C.W. Litton, D.C. Look, J.E. Hoelscher, B. Claffin, T.C. Collins, J. Nause, B. Nemeth, *J. Appl. Phys.* 95 (2004) 4802.
- [18] R. Triboulet, V. Munoz-Sanjósé, R. Tena-Zaera, M.C. Martinez-Tomas, S. Hassani, in: N.H. Nickel, E. Terukov (Eds.), *Zinc Oxide—A Material for Micro- and Optoelectronic Applications*, NATO Science Series II, vol. 194, Springer, Berlin, 2005, pp. 3–14.
- [19] D.C. Look, D.C. Reynolds, J.R. Sizelove, R.L. Jones, C.W. Litton, G. Cantwell, W.C. Harsch, *Solid State Commun.* 105 (1998) 399.
- [20] A. Janotti, C.G. Van de Walle, *Nat. Mater.* 6 (2007) 44.